2D stereotomography for anisotropic media

Steinar Nag[*,1,2], *Mathias Alerini*[1], *Eric Duveneck*[1] *and Bjørn Ursin*[2]
[1] *SINTEF Petroleum Research*
[2] *Norwegian University of Science and Technology*

Summary

Estimation of anisotropic velocity models is a challenging task. Different velocity estimation methods have been extended to include anisotropy, such as traveltime tomography and migration-based velocity analysis (MVA). This extension usually involves co-depthing of some key reflectors, which ensures the consistency of the estimated anisotropic models and adds constraints to the optimization. As a slope tomographic method, stereotomography offers an easier picking compared to traveltime tomography and is faster than MVA. It is also possible to include co-depthing in stereotomography. Stereotomography has not before been extended to anisotropic media.

We show here first results of velocity macro-model estimation by stereotomography for a 2D VTI medium using synthetic data. As an initial test, we invert for only one of the VTI parameter fields, using the exact models for the other parameter fields and the exact data. This inversion is done without any co-depthing. In each case, the estimated models show good fit with the exact models and encourage us to develop the method further.

Introduction

Stereotomography is a slope tomographic method (Sword, 1987) for estimating reference background velocity models and relies on the use of locally coherent events. The only assumption is that all the picked events are primaries. Stereotomography was first developed for 2D isotropic media with picking of PP events in the time domain (Billette and Lambaré, 1998). Later extensions of the method include isotropic PP/PS events (Alerini et al., 2002), 3D streamer data (Chalard et al., 2002), picking in the depth domain (Chauris et al., 2002; Nguyen et al., 2002), and picking in the poststack time domain (Lavaud et al., 2004). Using stereotomography provides the advantage of an easier picking compared to classical traveltime tomography methods, and is faster compared to MVA. However, stereotomography has not before been extended to an anisotropic medium. In such a case, not only the equations are more complicated, but the stability of the inversion is much more difficult, especially for obtaining consistent PP- and PS-migrated images. In other methods, this consistency is usually obtained by matching of the PP and PS events (Stopin and Ehinger, 2001; Foss et al., 2005).

After a brief summary of the method, we present the first results of anisotropic stereotomography.

Methodology

In stereotomography (Billette and Lambaré, 1998), locally coherent events are picked in the seismic data. The picked data associated with each event are the horizontal and vertical position of source and receiver, the two slopes at source and receiver (corresponding to the horizontal slowness, p_x^s and p_x^r) and the two-way traveltime T^{sr}. An iterative inversion is performed by minimizing the misfit between picked data and the data calculated by ray tracing in the current model. The model vector includes both velocity field parameters and the parameters of the pair of ray segments associated with each picked event. A joint optimization of ray segments and the velocity field is performed in each iteration.

In our implementation, we assume no error on the depths (z^s and z^r) of the sources and receivers to decrease the size of the inversion (Duveneck, 2004). This gives the data vector $\mathbf{d} = \left\{(x^s, x^r, p_x^s, p_x^r, T^{sr})_{i=1}^N\right\}$ and the model vector $\mathbf{m} = \left\{(x, z, \beta^s, \beta^r)_{i=1}^N, \left(C_{k=1}^{M_l}\right)_{l=1}^L\right\}$ for N locally coherent events (PP and PS). Here, (x, z) is the reflection/diffraction point in the subsurface, β^s and β^r are the two shooting angles towards the surface, and $\left(C_{k=1}^{M_l}\right)_{l=1}^L$ are L model fields (e.g. vertical velocities and anisotropic parameters), with each field described by M_l parameters (e.g. cubic B-spline knot values).

Extending stereotomography to an anisotropic medium requires the calculation of the Jacobian matrix (also called the Fréchet matrix), which includes the derivatives of all data parameters with respect to all model parameters. This Jacobian matrix can be computed by ray perturbation theory (Farra and Madariaga, 1987). It requires calculation of the derivatives in the phase space of the perturbations of the ray Hamiltonian. The Jacobian matrix is therefore much more complicated in anisotropic media than in isotropic media.

The estimation of anisotropy parameters is a highly underconstrained inverse problem. We could constrain the problem better by adding co-depthing of PP and PS key reflectors. We believe that the strategy given by Foss et al. (2005), in the context of differential semblance in angle, could also be used with stereotomography. In the present version of our code, co-depthing has not yet been implemented.

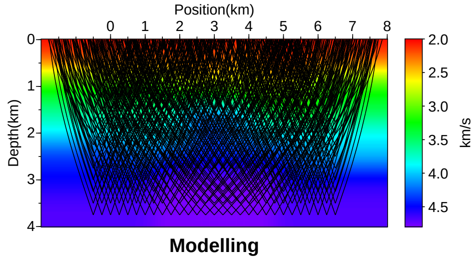

Fig. 1: Modelling of 377 PP data shown in the exact V_P model.

Synthetic examples

We defined smooth velocity models for the VTI parameters V_{P0}, V_{S0}, ε and δ , as defined by Thomsen (1986). The fields of the vertical velocities V_{P0} and V_{S0} were represented by 21×9 cubic B-spline knots in lateral and vertical directions respectively, with a knot spacing of 500 m in both directions. The ε and δ fields were represented by 6×5 cubic B-spline knots in lateral and vertical directions respectively, with a knot spacing of 2 km laterally and 1 km vertically.

Data were modelled by kinematic ray tracing using these velocity models. Fig. 1 shows the ray coverage of 377 PP ray pairs shot towards the surface from 29×13 reflection/diffraction points. The same points were used to shoot 377 PS events. The shooting angles were in the range $[22.5°, 45°]$.

As a first test of the validity of our code we estimated each of the fields V_{P0}, V_{S0}, ε and δ separately, using the exact models for the other three fields. The PP data were used to estimate V_{P0} and ε, while the SV-wave information in the PS data were used to estimate V_{S0} and δ. Figs. 2-5 show the results from separate estimation of V_{P0}, V_{S0}, ε and δ. The output model fits well to the exact model in each case.

Conclusions

We have presented first results of macro-model estimation by stereotomography in an anisotropic medium on synthetic data. The results show that our current anisotropic stereotomography code allows models to converge for all four Thomsen parameters in a 2D VTI medium, when estimating one Thomsen parameter field only. To further develop the method and invert for more than one parameter, we will add additional constraints by including co-depthing. In a joint inversion of VTI model parameters using co-depthing, both PP and PS data can be used when updating the model fields of each VTI parameter.

Acknowledgements

We thank Gilles Lambaré for fruitful discussions, and The Research Council of Norway for funding this work.

References

Alerini, M., Le Bégat, S., Lambaré, G., and Baina, R., 2002, PP and PS Stereotomography for a multicomponent dataset: 72nd Ann. Internat. Mtg., Soc. Expl. Geophys., Expanded Abstracts, 838–841.

Billette, F., and Lambaré, G., 1998, Velocity macro-model estimation from seismic reflection data by stereotomography: Geophys. J. Int, **135**, 671–690.

Chalard, E., Podvin, P., Le Bégat, S., Berthet, P., and David, B., 2002, 3D Stereotomographic inversion on a real data set: 72nd Ann. Internat. Mtg., Soc. Expl. Geophys., Expanded Abstracts, 946–948.

Chauris, H., Noble, M., Lambaré, G., and Podvin, P., 2002, Migration velocity analysis from locally coherent events in 2-D laterally heterogeneous media, part I: Theoretical aspects: Geophysics, **67**, 1202–1212.

Duveneck, E., 2004, Velocity model estimation with data-derived wavefront attributes: Geophysics, **69**, 265–274.

Farra, V., and Madariaga, R., 1987, Seismic waveform modeling in heterogeneous media by ray perturbation theory: J. Geoph. Res., **92**, 2697–2712.

Foss, S.-K., Ursin, B., and de Hoop, M., 2005, Depth-consistent reflection tomography using PP and PS seismic data: Geophysics, **70**, U51–U65.

Lavaud, B., Baina, R., and Landa, E., 2004, Automatic robust velocity estimation by poststack Stereotomography: 74th Ann. Internat. Mtg., Soc. Expl. Geophys., Expanded Abstracts, 2351–2354.

Nguyen, S., Noble, M., Thierry, P., and Baina, R., 2002, Tomography picking in the depth migrated domain using migration of attributes: 72nd Ann. Internat. Mtg., Soc. Expl. Geophys., Expanded Abstracts, 1140–1143.

Stopin, A., and Ehinger, A., 2001, Joint PP/PS tomographic inversion of the Mahogany 2D-4C OBC seismic data: 71st Ann. Internat. Mtg., Soc. Expl. Geophys., Expanded Abstracts, 837–840.

Sword, C., 1987, Tomographic determination of interval velocities from reflection seismic data: The method of controlled directional reception: Ph.D. thesis, Stanford University.

Thomsen, L., 1986, Weak elastic anisotropy: Geophysics, **51**, 1954–1966.

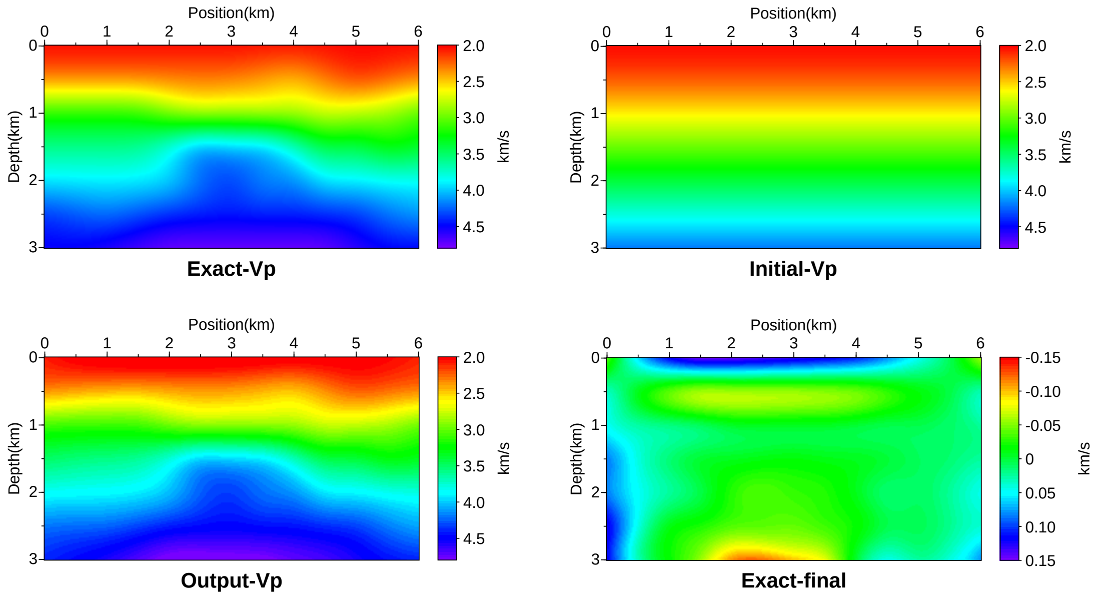

Fig. 2: Estimation of V_{P0}: exact model (upper left), initial model (upper right), final output model (lower left), and difference between exact and final models (lower right). The fixed V_{S0}, ε and δ models were the exact models in Figs. 3, 4 and 5, respectively. Only the central part of the model, where the ray coverage is good enough, is displayed. Some edge effects can be observed in the difference between exact and final output model.

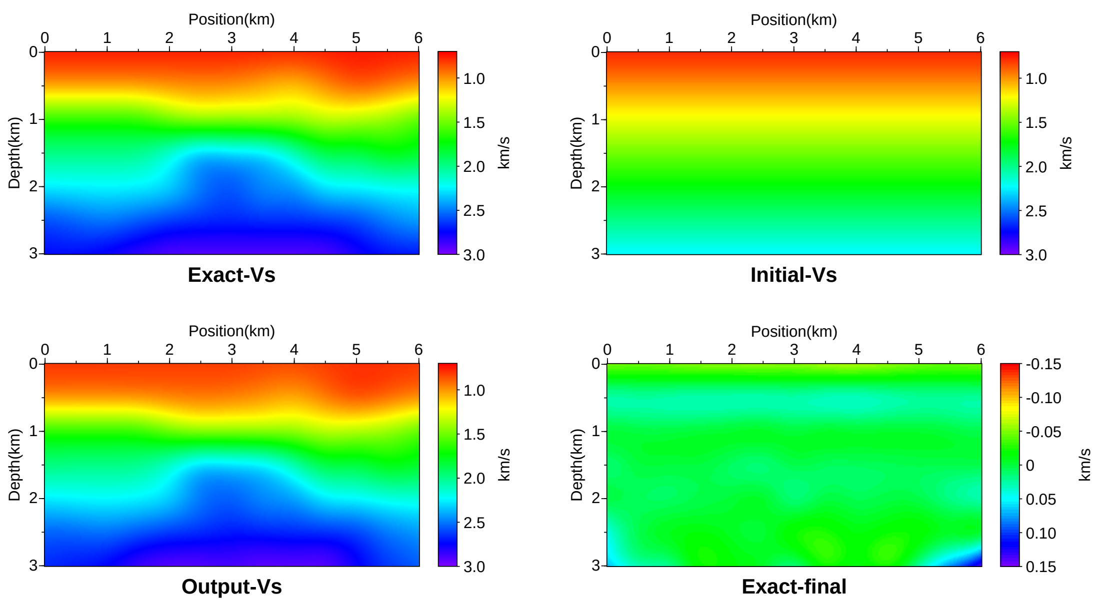

Fig. 3: Estimation of V_{S0}: exact model (upper left), initial model (upper right), final output model (lower left), and difference between exact and final models (lower right). The fixed V_{P0}, ε and δ models were the exact models in Figs. 2, 4 and 5, respectively. Only the central part of the model, where the ray coverage is good enough, is displayed. Some edge effects can be observed in the difference between exact and final output model.

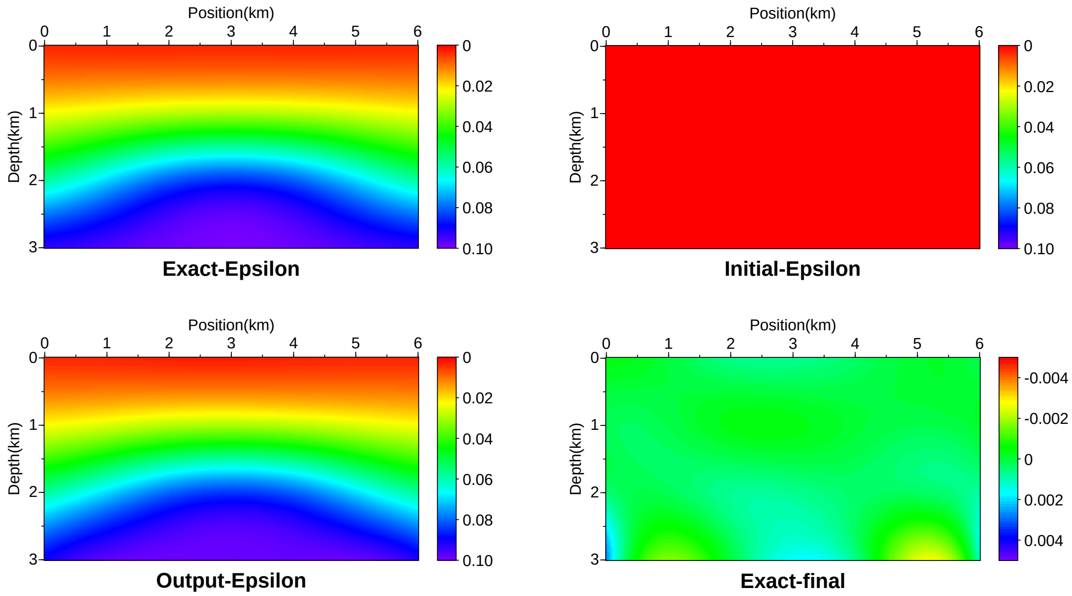

Fig. 4: Estimation of ε: exact model (upper left), initial model (upper right), final output model (lower left), and difference between exact and final models (lower right). Initially $\varepsilon = 0$. The fixed V_{P0}, V_{S0} and δ models were the exact models in Figs. 2, 3 and 5, respectively. Only the central part of the model, where the ray coverage is good enough, is displayed. Some edge effects can be observed in the difference between exact and final output model.

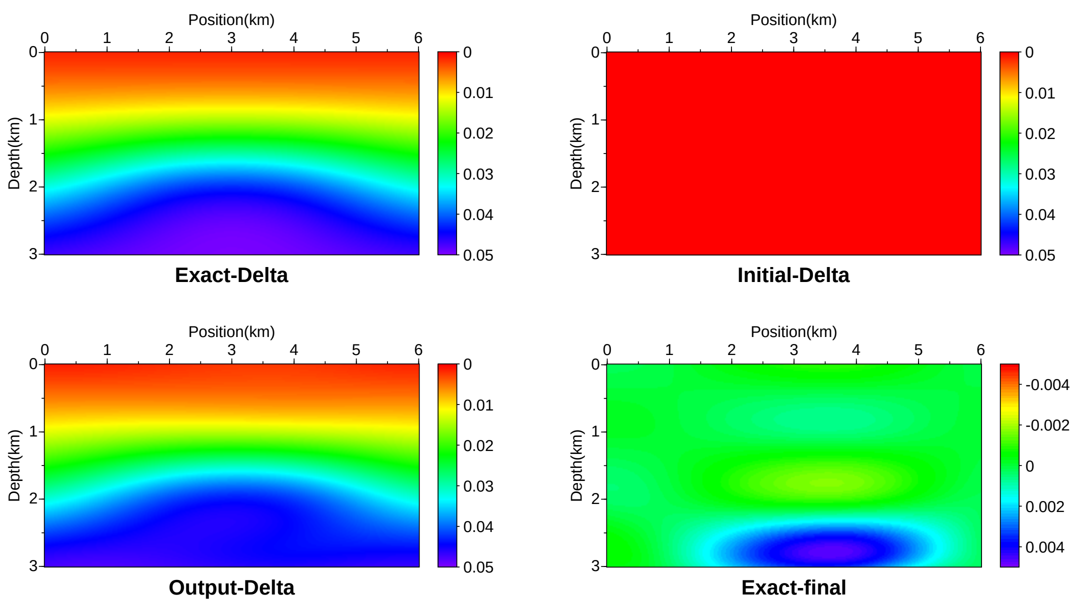

Fig. 5: Estimation of δ: exact model (upper left), initial model (upper right), final output model (lower left), and difference between exact and final models (lower right). Initially $\delta = 0$. The fixed V_{P0}, V_{S0} and ε models were the exact models in Figs. 2, 3 and 4, respectively. Only the central part of the model, where the ray coverage is good enough, is displayed. Some edge effects can be observed in the difference between exact and final output model.

EDITED REFERENCES

Note: This reference list is a copy-edited version of the reference list submitted by the author. Reference lists for the 2006 SEG Technical Program Expanded Abstracts have been copy edited so that references provided with the online metadata for each paper will achieve a high degree of linking to cited sources that appear on the Web.

REFERENCES

Alerini, M., S. Le Bégat, G. Lambaré, and R. Baina, 2002, PP and PS stereotomography for a multicomponent dataset: 72nd Annual International Meeting, SEG, Expanded Abstracts, 838–841.

Billette, F., and G. Lambaré, 1998, Velocity macro-model estimation from seismic reflection data by stereotomography: Geophysical Journal International, **135**, 671–690.

Chalard, E., P. Podvin, S. Le Bégat, P. Berthet, and B. David, 2002, 3D stereotomographic inversion on a real data set: 72nd Annual International Meeting, SEG, Expanded Abstracts, 946–948.

Chauris, H., M. Noble, G. Lambaré, and P. Podvin, 2002, Migration velocity analysis from locally coherent events in 2-D laterally heterogeneous media, part I, Theoretical aspects: Geophysics, **67**, 1202–1212.

Duveneck, E., 2004, Velocity model estimation with data-derived wavefront attributes: Geophysics, **69**, 265–274.

Farra, V., and R. Madariaga, 1987, Seismic waveform modeling in heterogeneous media by ray perturbation theory: Journal of Geophysical Research, **92**, 2697–2712.

Foss, S.-K., B. Ursin, and M. de Hoop, 2005, Depth-consistent reflection tomography using PP and PS seismic data: Geophysics, **70**, U51–U65.

Lavaud, B., R. Baina, and E. Landa, 2004, Automatic robust velocity estimation by poststack stereotomography: 74th Annual International Meeting, SEG, Expanded Abstracts, 2351–2354.

Nguyen, S., M. Noble, P. Thierry, and R. Baina, 2002, Tomography picking in the depth migrated domain using migration of attributes: 72nd Annual International Meeting, SEG, Expanded Abstracts, 1140–1143.

Stopin, A., and A. Ehinger, 2001, Joint PP/PS tomographic inversion of the Mahogany 2D-4C OBC seismic data: 71st Annual International Meeting, SEG, Expanded Abstracts, 837–840.

Sword, C., 1987, Tomographic determination of interval velocities from reflection seismic data: The method of controlled directional reception: Ph.D. thesis, Stanford University.

Thomsen, L., 1986, Weak elastic anisotropy: Geophysics, **51**, 1954–1966.